Flinders
UNIVERSITY

Dynamical (e,2e) Studies of Bio-Molecules

Joseph Douglas Builth-Williams

Submitted in fulfillment for the requirements
of the degree of Masters of Science

March 2013

School of Chemical and Physical Sciences
Flinders University of South Australia

Science is a way of thinking much more than it is a body of knowledge.

∼ Carl Sagan (1934-1996)

5

Measurements on α-Tetrahydrofurfuryl Alcohol

5.1 Introduction

α-Tetrahydrofurfuryl Alcohol (THFA), otherwise known as tetrahydro-2-furanmethanol or oxolan-2-methanol, is a hetrocyclic organic compound. It is closely related to the dioxane, pyrrolidine and furan heterocycles and is derived from tetrahydrofuran (THF). THFA has the chemical formula $C_5H_{10}O_2$, a vapour pressure of 2.3 torr (at 39°C) and a density of 1.053 g/cm^3. The boiling point of THFA is 446K, its melting point is 193K and at room temperature it is a colourless liquid. Much like THF, THFA is made up of a five member ring, with a single oxygen occupying the first position. A single carbon chain, connected to a hydroxyl group, is attached to the fifth carbon position (see Figure 5.1).

5.1.1 Significance of this Molecule

DNA, being one of the most important molecules for life (see Section 1.2), is made up of a number of different components. THFA can be considered as being one of those components, as should be apparent from Figure 5.1 which also depicts a segment of the sugar-phosphate backbone of a single DNA strand. The fragment containing the THFA molecule is clearly defined in this figure.

There have been a number of studies into deoxyribose analogue molecules, such as THF, THFA and 3-hydroxytetrahydrofuran (3HTHF). These molecules have been studied with various techniques, including measuring the elastic DCSs of THF [116, 117, 118, 119], THFA [120] and 3HTHF [121, 122]; the total cross sections for electron and positron scattering of THF [123, 124, 125], THFA

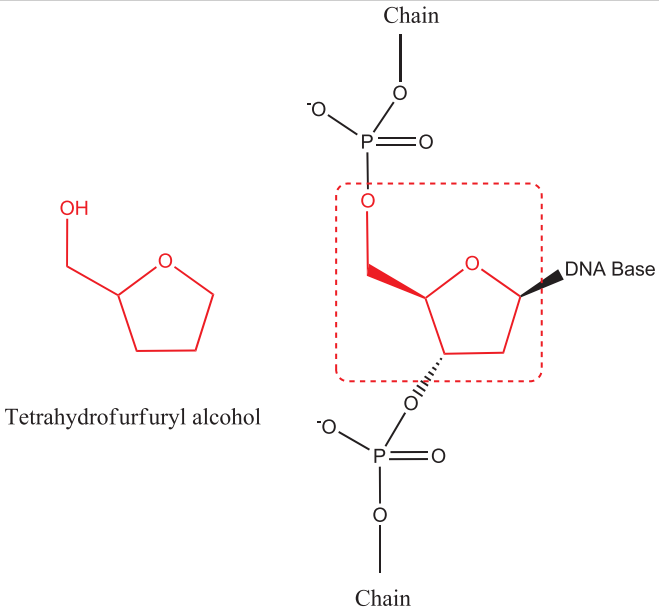

Figure 5.1: *The structure of THFA, and a segment of the sugar-phosphate backbone of DNA, highlighting the THFA molecule [38].*

[126, 127] and 3HTHF [128]; and even an earlier dynamical (e,2e) measurement on THF [36].

5.2 Binding Energy Spectrum

The Binding Energy Spectrum (BES) of THFA, in the range of 8-12eV, is shown in Figure 5.2, and is the result of numerous measurements taken over a long period. All those measurements were made under the same kinematic conditions: 250eV incident electrons and 20eV ejected electrons were measured with the scattered and ejected analysers being held at $-10°$ and $90°$, respectively. The scattered electron energy was scanned across a range of energies at 0.3eV steps, and using coincidence measurement techniques the BES was determined.

The BES has been fitted with three Gaussian functions, which have been labelled according to the orbitals they represent. The orbital assignment is based upon the experimental PES measurements collected by Ibănescu *et al.* [129], as well as theoretical calculations performed using the Outer Valence Green's Function (OVGF) model (and initialised using the DGTZVP basis set [130]), as seen in Table 5.1. A complete table of the results of the fitting algorithm can be seen in Table A.6 in Appendix A.

The coincidence energy resolution for the (e,2e) spectrometer was estimated in

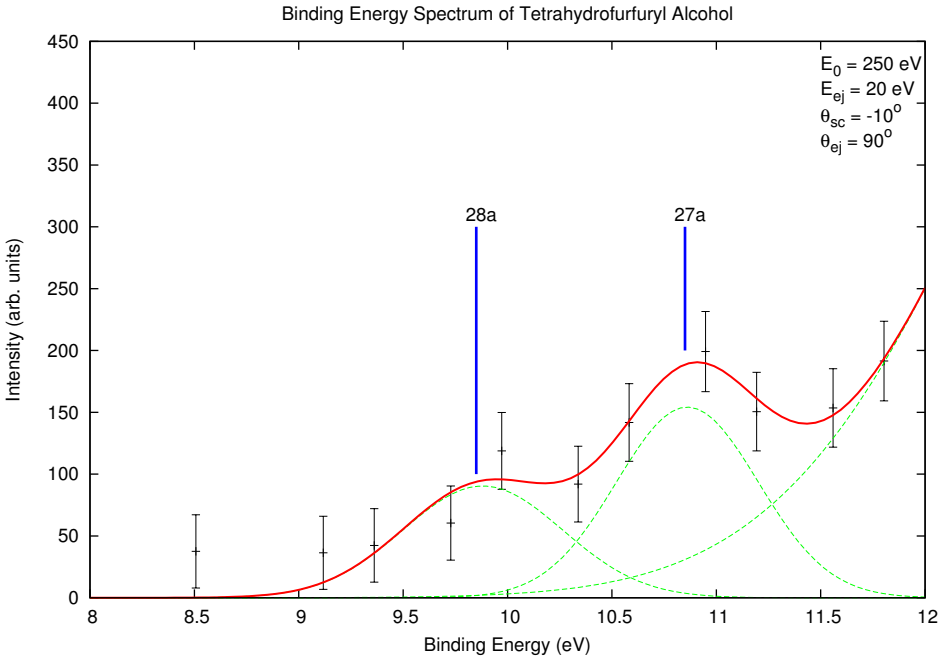

Figure 5.2: *The complete Binding Energy Spectrum of α−Tetrahydrofurfuryl Alcohol in the range of 8-12eV. The HOMO (28a) and NHOMO (27a) are labelled, while the leading edge of the third Gaussian is associated to the 26a orbital.*

Table 5.1: *Ionisation potentials of THFA in eV, collected by Ibănescu et al. [129]. The (e,2e) column is data from the current work.*

Orbital	PES (eV)	OVGF/DGTZVP (eV)	(e,2e) (eV)
28*a*	9.81	9.79 (0.91)	9.8
27*a*	10.60	10.93 (0.91)	10.7
26*a*		11.47 (0.91)	
25*a*		11.86 (0.91)	
24*a*		12.09 (0.91)	
23*a*		12.41 (0.91)	
22*a*		13.24 (0.91)	
21*a*		14.03 (0.91)	
20*a*		14.37 (0.91)	
19*a*		14.65 (0.90)	
18*a*		15.62 (0.91)	
17*a*		16.39 (0.90)	

this case to be 1.1eV, based upon the width of the helium 1*s* orbital measured under the same kinematic conditions. The width of the various Gaussian functions, used in the fit to Figure 5.2, was a convolution of the instrumental energy resolution and the natural orbital shell widths (Γ), which were obtained from the PES data. As a consequence of the limited coincidence energy resolution of the (e,2e) spectrometer, the HOMO was unable to be completely resolved from the Next Highest Occupied Molecular Orbital (NHOMO). Nonetheless, as

Figure 5.2 demonstrates, contamination from the $27a$ orbital in regard to that of the HOMO should be relatively small although non-zero.

5.3 Experimental Considerations

Much like pyrimidine, the THFA sample was purchased from Sigma-Aldrich at a stated purity of 99%. It should be noted that when this sample was transferred to the sample vessel, it was exposed to the air and so may have been contaminated. As such, three freeze-pump-thaw cycles were performed (see Section 4.3) in order to remove any potential gaseous contaminants.

Also, much like for pyrimidine, THFA is a volatile liquid and so to achieve a molecular beam of sufficient density at the interaction region, the sample needed only be exposed to a vacuum. However, there were issues with THFA condensing within the chamber, specifically around the molecular beam capillary, which caused pressure fluctuations. This challange was overcome in much the same way as it was for pyrimidine, by gentley heating the capillary as well as the chamber (see Section 3.1.5).

Another consideration to take into account is the particular conformation of the THFA molecule during the experiment. Twenty possible conformations for THFA exist, when it is in the gas phase, due to out-of-plane puckering vibrations which causes the phase of the puckering to rotate around the ring [131]. The molecular structure of THFA in gas phase has previously been investigated by electron diffraction [132], and it was found that the sample was dominated by two conformers with abundances of $84 \pm 8\%$ and $16 \pm 8\%$. In these conformers, the O-H group of the THFA molecule is directed towards the oxygen on the ring, and appears to be stabilised by hydrogen bonding [132].

5.4 Results and Discussion

Presented in Figure 5.3 are the experimental and theoretical TDCS results for the HOMO of THFA. All three plots were measured using 250eV incident electrons and 20eV ejected electrons. The scattered analyser was held at -5°, -10° or -15° while the ejected analyser was moved over a range of angles, in 5° steps. The total range of angles covered by the ejected analyser varied depending upon the actual angle the scattered electron analyser was being held at, due to the physical limitations imposed by the (e,2e) spectrometer (see Section 3.1.4).

As mentioned earlier in this thesis, the experimental TDCS measurements are

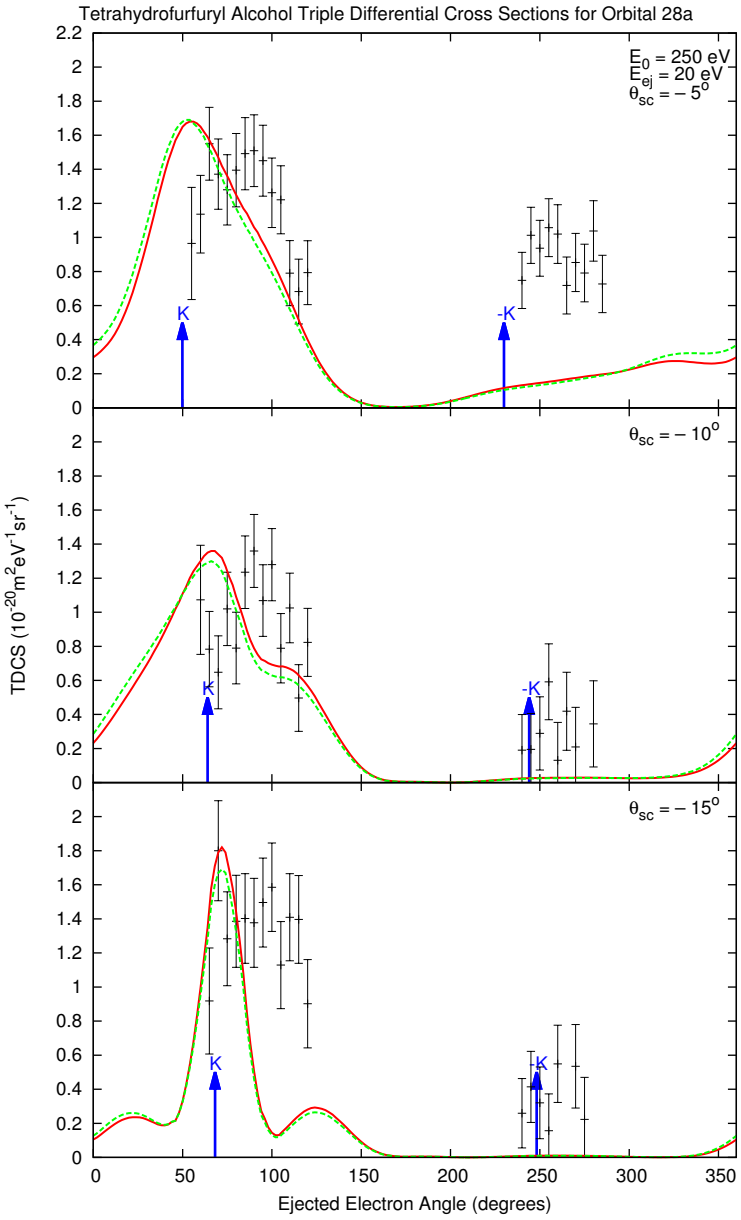

Figure 5.3: *TDCS of the 28a orbital of α−Tetrahydrofurfuryl Alcohol, measured respectively at the scattered electron angles of* $-5°$, $-10°$ *and* $-15°$, *where* $E_0 = 250$ *eV and* $E_{ej} = 20$ *eV. The solid red line represents the M3DW results, while the green dotted line represents the DWBA results.*

relative and have been normalised for each θ_{sc} to the M3DW calculations in order to give the best visual fit to the theory in the binary region. Tables for this experimental data can be found in Appendix A, in particular Tables A.7, A.8 and A.9.

Two sets of theoretical results have been provided alongside the experimen-

tal data: the solid red line represents the results from the M3DW calculations, while the green dashed line represents the results from the DWBA calculations. These calculations were performed by Madison *et al.* [115]; further information about the model can be found in his previous work [36, 75] as well as in Section 2.5.3. As discussed in Section 2.5.3, the difference between the M3DW and DWBA calculations is essentially that the M3DW calculation includes Post Collision Interaction (PCI) terms to all orders for the ejected and scattered electrons. A qualitative observation of the M3DW and DWBA results for the HOMO of THFA, shows that there is little to no difference between the two. This suggests that the PCI terms are having little effect in the current kinematic setup for the HOMO. Contary to this, however, the experimental binary and recoil peaks are shifted from κ and -κ, respectively. Such a result would be consistent with PCI playing a role in the collision dynamics.

Table 5.2: *The current binary to recoil peak (B-R) ratios found in the present study for THFA.*

Angle	B-R ratio	Error
5°	1.677	±0.413
10°	2.680	±1.402
15°	2.491	±1.464

The binary peaks of the experimental measurements for all three TDCSs are rather broad, an observation which appears to be common for a number of molecular targets. In particular, the TDCSs of the THF HOMO similarly presented with broad binary peaks under very similar kinematic conditions [36]. However this is largely unsurprising due to the similar structure that both molecules share, as THFA can be considered to be a derivative of THF. In contrast to THFA, pyrimidine [37] and thymine [133] both exhibit rather narrow binary peaks. This particular observation may reflect the molecular structure of the six member aromatic rings that make up pyrimidine and its derivative thymine.

In the first panel of Figure 5.3 (i.e. $\theta_{sc} = -5°$) the experimental recoil peak is of a relatively larger magnitude compared to the second ($\theta_{sc} = -10°$) and third ($\theta_{sc} = -15°$) panels. While the theoretical calculations predict a larger recoil peak for the scattered electron angle of $-5°$, compared to those at $-10°$ and $-15°$, they significantly underestimate the magnitude of those recoil peaks when compared to the experiment. This is a common observation across all three scattered electron angles investigated, suggesting that the nuclear scattering strength used in the calculations was probably insufficient, as the recoil

peak magnitude is usually indicative of electron scattering from the molecular nucleus. Another point of interest from Figure 5.3, is that the recoil peaks in THFA are of a smaller magnitude when compared to the TDCS behaviour found in molecules such as H_2O. Indeed H_2O has a binary peak to recoil peak ratio close to unity [30], while a number of other molecules such as THF [36], CHCOOH [35] and pyrimidine [37] have displayed a larger ratio. As previously mentioned in Section 4.4, there have been two explanations put forward to explain this particular observation:

i) Colyer *et al.* [35] suggested that this observation may arise due to a lack of a nuclear charge at the centre-of-mass for the molecule; while

ii) Xu *et al.* [114] suggested that the observed binary-recoil ratio are caused by the specific symmetry of the probed orbital in each species.

More recently, the MST group have changed their approach so that they now calculate a TDCS for each molecular orientation, before averaging those results in order to mimic the spherical averaging of the experiment [78]. While their results for CH_4 are only preliminary, larger recoil peaks, relative to the binary peak, were found in each kinematic case studied.

A further feature of note in Figure 5.3 is the suggestion of a local minimum in the TDCS at the scattered electron angle $-10°$, in the binary peak, located at around the momentum transfer vector, $\vec{\kappa}$. As mentioned in Section 2.4.2, this local minimum occurring around $\vec{\kappa}$ is indicative of a p-type molecular orbital, which is consistent with results from quantum channel calculations for the HOMO [38]. However this minimum, in the TDCS for the binary peak, is less evident at $\theta_{sc} = -15°$ where it might be expected to be much more pronounced, as this is closer to the Bethe ridge kinematics. A quantitative explanation for this, and some of the other experimental and theoretical inconsistencies, at this time remains elusive.

5.5 Conclusion

In this chapter experimental and theoretical dynamical (e,2e) results were presented for THFA. THFA acts as a good analogue for the sugar-phosphate backbone that is absolutely essential for DNA, and thus life. By studying the TDCS of THFA, it is hoped that a better model for the effects of radiation on biological matter might ultimately be developed.

The current TDCS measurements were performed with 250eV incident electrons and 20eV ejected electrons. The scattered electrons were measured at the

angles $-5°$, $-10°$ or $-15°$ for the $28a$ (HOMO) orbital of THFA. Broad binary peaks were observed at all the scattered electron angles, with only the hint of a suggestion for a double-lobe structure that is expected from a 'p-type' molecular orbital such as the $28a$ orbital. The two theoretical calculations (M3DW and DWBA) also predicted broad binary peaks for $\theta_{sc} = -5°$ and $-10°$, but predicted a narrow binary peak for $\theta_{sc} = -15°$. This latter result was not supported by the experimental results.

For the scattered electron detection angles of $-10°$ and $-15°$, a quite small recoil peak was observed relative to the binary peak. However at the scattered electron detection angle of $-5°$, the recoil peak was relatively large suggesting that there was significant electron interaction with the target ion at that specific kinematic condition.

The differences between the DWBA and M3DW results were slight, suggesting that PCI has a minimal effect for the $28a$ orbital under the present kinematics. However, in an apparent contradiction, the experimental results were observed to exhibit a shift in the binary peak position away from the momentum transfer vector, $\vec{\kappa}$. This would suggest that PCI is playing a more significant role in the collision dynamics than the M3DW results predict.

Overall, the theoretical calculations performed using the M3DW and DWBA methods were found to be in marginal to fair agreement with the observed experimental results. This state of affairs may be due to the complexity of the molecular target for the calculations to accurately represent, or problems with the molecular averaging used in the theory to mimic the random molecular orientation of the target molecules in the measurements. A small discrepancy, introduced by some NHOMO contribution to the HOMO coincidence signal, due to the present energy resolution, also cannot be ruled out.